ICSV14
Cairns • Australia
9-12 July, 2007

THE HEAD RELATED TRANSFER FUNCTION SIMULATION BY FEM/IEM AND RECIPROCAL THEOREM

Hiroshi Muraoka[1], Yuta Takahashi[1], Tubagus Haedar[1], Makoto Otani[2] and Tatsuya Hirahara[2]

[1]Research Center of Computational Mechanics, Inc.
Togoshi NI-Bldg. 1-7-1 Togoshi, Shinagawa-ku, Tokyo, 142-0041, Japan
muraoka@rccm.co.jp
[2]Department of Intelligent Systems Design Engineering
Toyama Prefectural University, Imizu City, Toyama, 939-0398, Japan

Abstract

An effective method of reducing computational cost involving Head Related Transfer Function (HRTF) simulation for high frequency is to apply the reciprocal theorem. Commonly, the Boundary Element Method is used since both calculation and mesh generation effort are minimal, however it is sensitive to geometry complexity and unstable during the discretization of the reciprocal theorem. Hence, in order to eliminate the errors and increase the efficiency of the outcome, this report demonstrates a new approach to Head Related Transfer Function (HRTF) simulations by coupling Finite Element Method (FEM) with Infinite Element Method (IEM). First, the validity of the reciprocal theorem was examined by comparing numerical results along with the impulse response up to 1000Hz. Once the accuracy has been established, further studies were carried out between 10 and 20KHz to illustrate the practicability of this method.

1. INTRODUCTION

HRTF describes how a particular sound wave is filtered by the diffraction and reflection of facial features before reaching the eardrum. It is quite essentially how we identify a sound and it is affected by our individual facial characteristics (head, nose, ear, cheekbone) along with the position and strength of the sound source. Due to computational improvement over the years, higher frequency calculations are no longer out of reach. Although being restricted to homogeneous problems and without uniqueness in the solution, BEM [1] has been considered as a reference method since it offers reduction in dimensionality and the fact that it handles the sound radiation at the far field rigorously.

When retorting FEM [2], two methods are considered; one is FEM/IEM and the other is DtN-FEM. Domain-based methods such as FEM/IEM are more suitable for solving exterior acoustic problems than the ones based on DtN [3] due to the sparse matrices problem and efficient solution procedures such as parallel calculations (frequency and domain wise). Coupling FEM with IEM will enable a natural extension of finite element to an unbounded

domain. FEM was utilized, as it is not affected by geometrical complexity since it is based on the weak variational formulation and sound hard condition is automatically accounted as a natural boundary condition. Although the FEM offers high accuracy results, it is well known that the computational load is heavy due to the need of discretization of the whole computational domain (large stiffness matrix). For instance, regarding high frequency simulations, the elements around the head, sound source and within the volumetric space need to be refined in a manner to capture the wavelength of the monopole, which culminates in a fine grid generation, increased computational time and memory usage. Integrating the reciprocal theorem to the FEM/IEM does not only solve the dimensional issue but also facilitates the process of obtaining the output, such as directivity, as unlimited number of observation points can be placed into a single calculation.

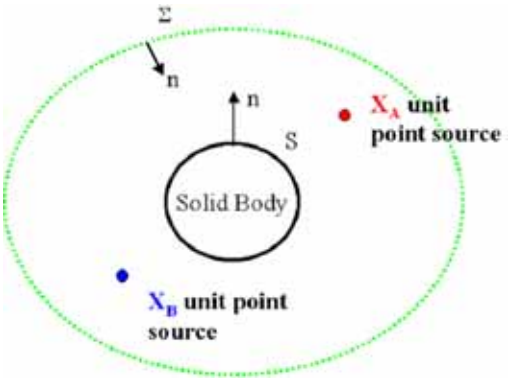

Figure 1. Two acoustic problems diagram

Consider a case in which a particular sound of frequency is generated by two unit point sources around a solid body *S*. The reciprocal theorem [4] would indicate that sound pressure obtained at B from a source at A is equal to one obtained at A from a source at B as follows

$$G(x_A, x_B, \omega) = G(x_B, x_A, \omega) \tag{1}$$

The functional forms of the respective velocity potentials generated by the two sources are as follows

$$\textit{Sound pressure from A satisfies } (\Delta + k^2)G(x, x_A, \omega) = \delta(x - x_A) \tag{2}$$

$$\textit{Sound pressure from B satisfies } (\Delta + k^2)G(x, x_B, \omega) = \delta(x - x_B) \tag{3}$$

$$\textit{Wave number}, k = \frac{2\pi f}{c} \tag{4}$$

This theorem aids the process of computational reduction by minimizing the analysis domain, which is highlighted in this paper. This paper is organized as follows: After this introduction, the governing equations for the weak variational formulation are presented in section 2. Section 3 outlines the problem definition and section 4 shows some numerical results. The penultimate section discusses high frequency results and the final section summarizes the work carried out and identifies future guidance for improvements.

2. GOVERNING EQUATIONS

Finite Element Method provides calculation stability compared with Boundary Element Method, as it is not affected by the complexity of the model structure. The FEM is used to discretize the bounded domain between the head model and the infinite boundary [5]. HRTF is a problem of solving scattering sound waves by a head model (scattering body) from a unit source at a certain point in space. In order to visualize this, the Helmholtz equation including non-homogeneous term creating the incident wave must be solved as an outgoing wave at infinity.

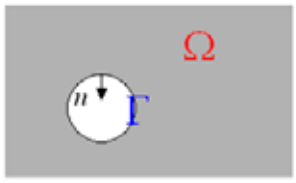

Figure 2. Acoustic boundary domain

$$\nabla^2 p + k^2 p = g \qquad \text{in } \Omega \tag{5}$$

$$\nabla p \cdot n = 0 \qquad \text{on } \Gamma \tag{6}$$

$$\frac{\partial p}{\partial r} + ikp = O\left(\frac{1}{r^2}\right) \tag{7}$$

Ω represents an unbounded domain and Γ its boundary. Forcing function is represented by g, n is the outward unit normal vector on the boundary and r is the reference distance. ACTRAN's conjugated infinite element provides both high accuracy and flexibility in modeling radiation problems. Based on multipole expansions in spherical or spheroidal or ellipsoidal coordinates system, the infinite element can accommodate any geometry and arbitrary radial interpolation orders while remaining stable [6].

3. PROBLEM DESCRIPTION

Evaluation step for the reciprocal theorem were divided in two folds; case A had the sound source inclined 45 degrees to the right at 0.5m with the recipient point being next to the right ear, whereas case B had the exact opposite settings as illustrated below

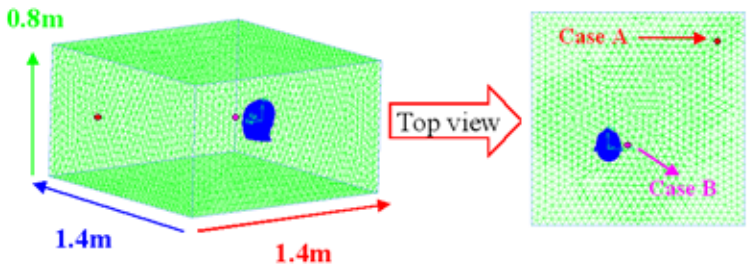

Figure 3. Mesh structure and sound source/recipient point location

Mesh comprised of 70000 nodes with 330000 tetrahedral elements, suitable for analysis up to 1000Hz and the head model was obtained from MRI scan (shown below), which had a hight of approximately 0.25m with a 0.1m radius.

Figure 4. Head model and boundary condition of the room

To demonstrate the fact that the efficiency will not be lowered by the diffraction effect within the computational domain, both cases were tested again with a reflective wall set on the left hand side of the room. Simulations were carried out for frequencies between 50Hz to 1000Hz in the goal of obtaining the impulse response and outline any numerical variation between the cases.

4. NUMERICAL COMPARISON

Efficiency of the reciprocal theory was first tested utilizing two separate cases, one by placing a monopole away from the head model having the receiving point next to the right ear and the second case exactly the opposite to the first. Comparison was carried out across a frequency band of 50 to 1000Hz at 50Hz interval

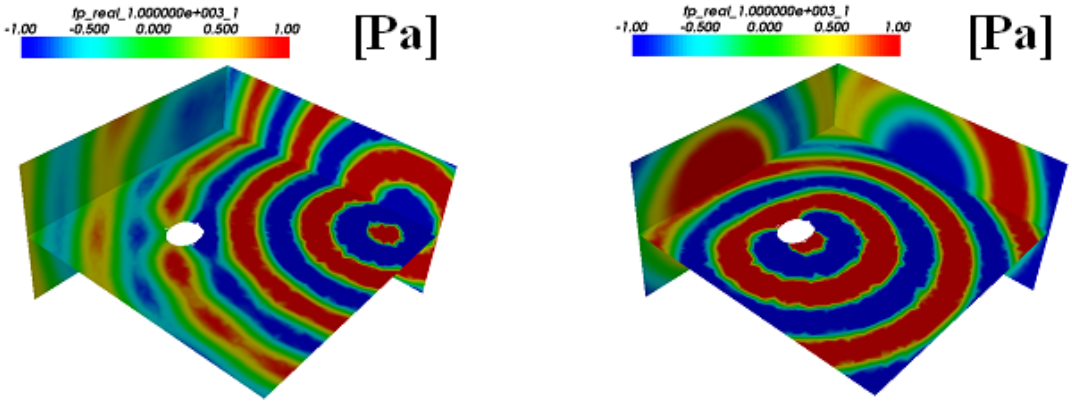

Figure 5. Sound propagation patterns for case A and B at 1000Hz

It can clearly be observed that the pressure waves are generated from the monopole sound source and the head diffracts its patterns. The overall sound strength within the room differs due to the position of the sound source; one being close to the FE/IE boundary and the other close to the head model. Although the outcome from a contour point of view differed, analysing real and imaginary figures at each recipient point respectively across the frequency range at 50Hz interval were very closely matched as shown in the following page (figure 6). The following step was to determine the level of deviation present in the numerical solution.

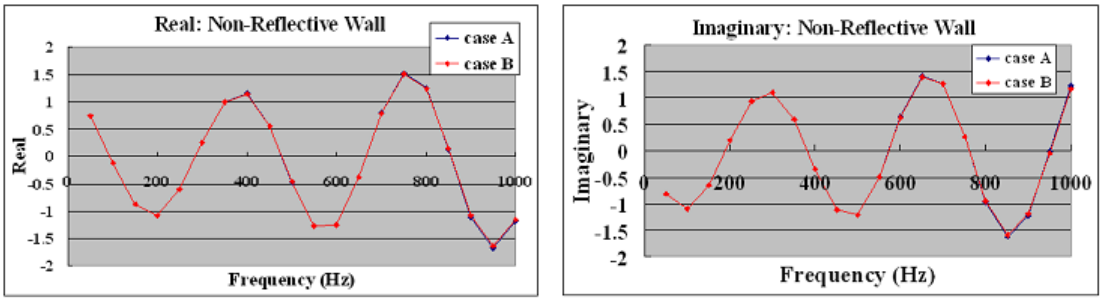

Figure 6. Real and Imaginary comparison between case A and B (Pa)

Quantitative error estimation of the result reiterated that error margin rises after reaching a certain frequency but up to 600Hz (approximately 10 element per wavelength), the solution is fairly stable. This relation is due to the fact that the grid has been created to contain 6 elements per wavelength and reaching the optimum frequency tends to affect the accuracy of the numerical solution as seen for both amplitude and phase error margin in figure 7.

$$Amplitude\ error\ (e_A) = \frac{Amplitude_{No\ reciprocal} - Amplitude_{with\ reciprocal}}{Amplitude_{No\ reciprocal}} \tag{8}$$

$$Phase\ error\ (e_P) = \left[\phi_{No\ reciprocal} - \phi_{with\ reciprocal}\right] * 180 / \pi \tag{9}$$

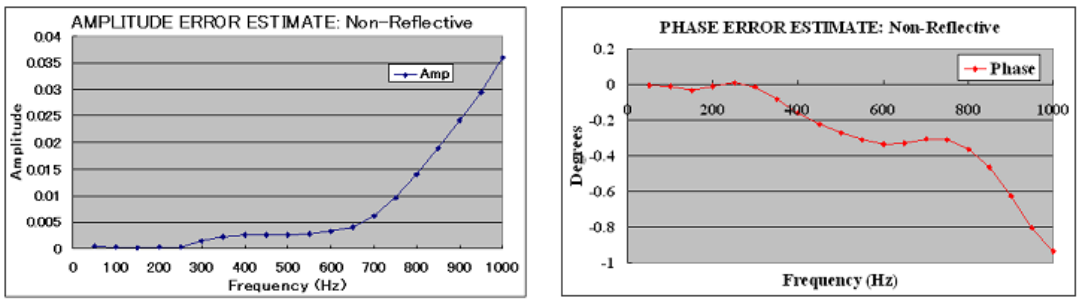

Figure 7. Amplitude and Phase error estimate for non-reflective case

For further verification of the stability of the solution, the left hand side of the room was set as a reflective wall. Adding the extra boundary condition affected both real and imaginary values as shown below (figure 8). A small irregularity is seen around the 800Hz region but as in the previous non-reflective case, most of the points are identical.

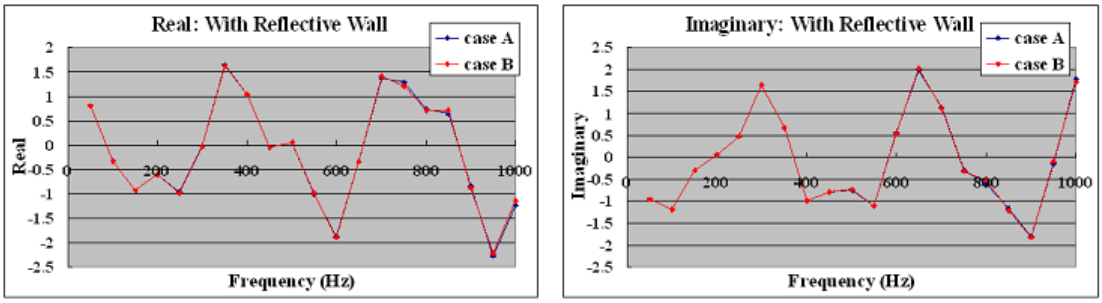

Figure 8. Real and Imaginary comparison between case A and B with reflective wall (Pa)

Error estimate study displayed a significant instability of the numerical solution at 800Hz for both amplitude and phase values. Again, similar reasoning regarding element size was deducted for this problem, hence we believe refining the grid further or increasing the radial interpolation order could diminish the error magnitude.

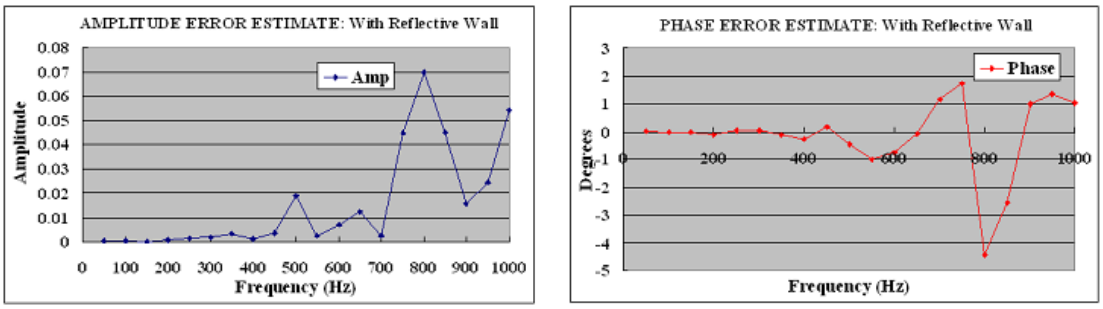

Figure 9. Amplitude and Phase error estimate for reflective wall case

The corresponding impulse response between the default and reflective wall case with the sound source inclined at 45 degrees toward the right are shown below for practical purpose. It is clear that the sound wave reaches the right ear first in the default case, as the source is closer to it compared to the left ear.

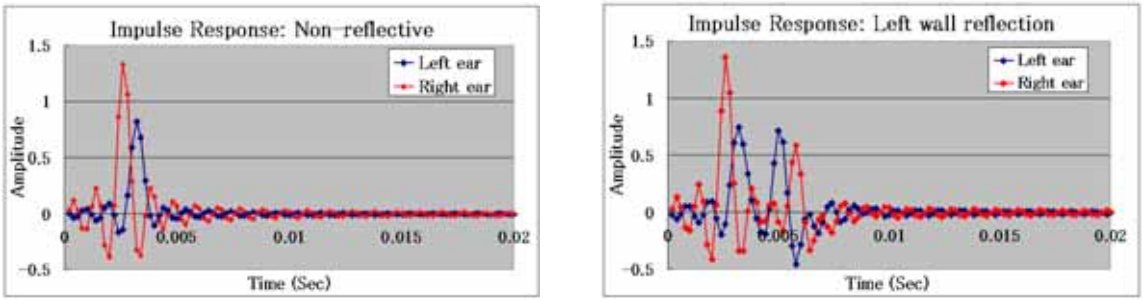

Figure 10. Impulse response for cases with sound source away from the head (Pa)

The effect of the reflective wall is seen on the right graph as the second sound wave reflected by the wall reaches the left ear first. Culmination of the results so far proves the validity of the reciprocal theory hence, the analysis moved on to higher frequency, which were deemed impractical without heavy machine power.

5. HIGH FREQUENCY STUDY

The head model was placed inside a sphere of 0.17m radius with a monopole set next to the left ear at a frequency range of 10 to 20 KHz. The element size had to be restrained to one sixth of the wavelength (2.8mm) hence a dense grid of approximately 300000 nodes and 1.6million elements had to be computed. As a reference, this case was operated on a machine with Dual-Core Opteron 2218 (2.6GHz) processor with 8GB memory and took approximately 50 minutes for one frequency calculation. Directivity and the dip characteristics of sound pressure level at 1.5 meter radius around the head model (horizontal plane to the ears) were determined across the relevant frequency. Figure 11 demonstrates how the FE/IE boundaries were divided for the sound source and the recipient point, where the computational domain (FE) is kept to a minimum. IE governs the outer boundary and observation points were placed at a 5 degrees

interval on the circle with 1.5 meter radius from the center coordinate (total of 72 observation points).

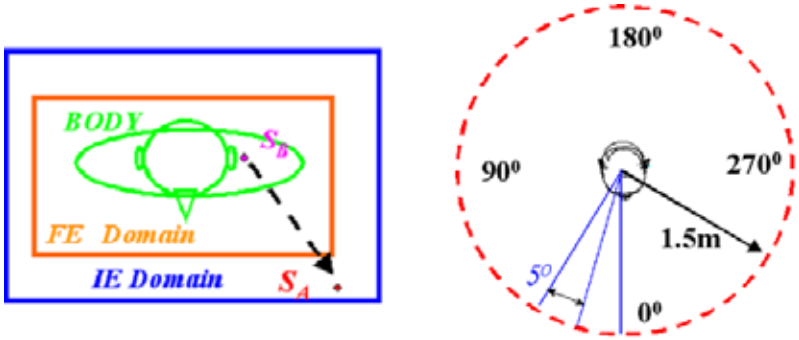

Figure 11. Domain boundary and observation perimeter

As the monopole is placed near the left ear, only a weak portion of sound wave reaches the right hand side, which results in low sound pressure level compared to the left region being illustrated in figure 12. Also, decreasing the wavelength increased the diffraction effect.

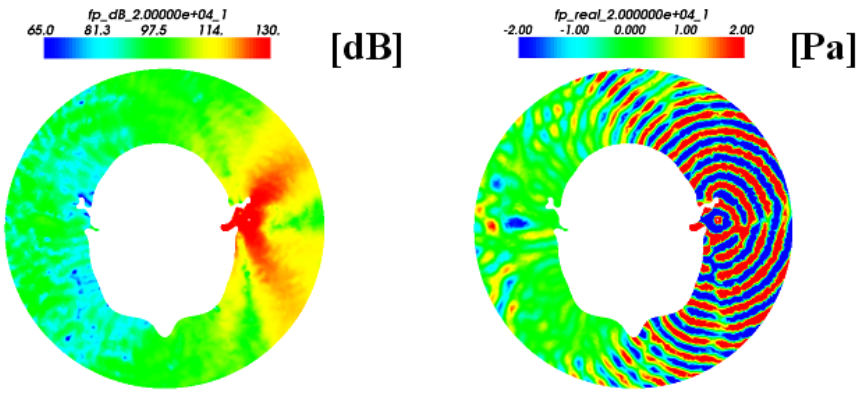

Figure 12. Sound pressure Level and Real Part contour at 20KHz

The directivity reiterated that the strongest sound region is constantly around the front left region regardless of the frequency, thus the HRTF variation will always be higher between 180-360 degrees compared to the 0-90 degrees plane.

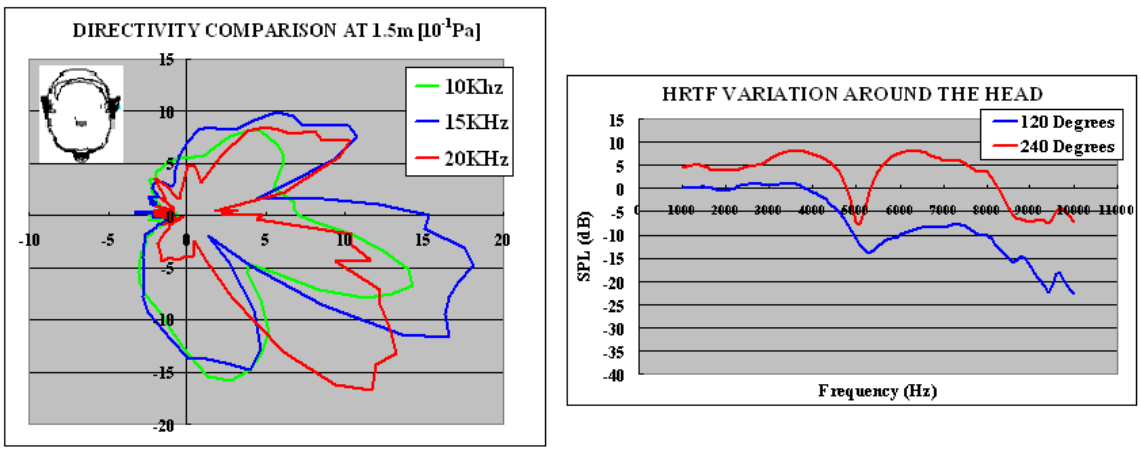

Figure 13 Directivity and HRTF variation characteristics

6. CONCLUSIONS AND FURTHER WORK

The reciprocal theory application was successful in terms of numerical accuracy and it was not affected by the addition of extra reflective property. Also, the sound propagation pattern and the impulse response suggested that the coupling with FEM produced logical results by eliminating the potential frequency dependent calculation instability. Complexity of the analysis structure was negligible (facial characteristics) and as unlimited monitor points (recipient points) could be placed within a single calculation, determining the directivity is simple. Overall, the coupling analysis managed to reduce computational time considerably by minimizing the analysis domain without affecting the efficiency of the result. The next step would be to compare simulation efficiency to that of experimental to further validate the feasibility of FEM/IEM coupling with reciprocal theory. Calculation at higher order of frequency and addition of extra boundary condition such as impedance could be of interest.

REFERENCES

[1] M. Otani and S. Ise, "A fast calculation method of the head-related transfer functions for multiple source points based on the boundary element method", *Acoust. Sci. & Tech* **24**, 5 (2003).

[2] Free-Field-Technologies-S.A., *Actran 2006 Aeroacoustic Solutions: Actran/TM and Actran/LA - User's Manual* , Belgium, 2006.

[3] Y. Naka, A.A. Oberai and B.G Shinn-Cunningham " The finite element method with the Dirichlet-to Neumann map for sound-hard rectangular rooms" *Proc. 18th Int. Congr. Acoustics*, **Vol. IV**, pp. 2477-2480 (2004).

[4] M.S. Howe, *Theory of Vortex Sound*, CAMBRIDGE UNIVERSITY PRESS, 1992.

[5] F. Ihlenburg, *Finite Element Analysis of Acoustic Scattering*, Springer, 1998

[6] R.J. Astley, G.J. Macaulay and J.P. Coyette, "Mapped wave envelope elements for acoustic radiation and scattering", *JSV*, **170** (1), 97-118 (1994)

[7] M. Otani and S. Ise, "Head Related Transfer Function Analysis and Application", *Journal of Acoustical Society of Japan* **61**, 404-409 (2005)

[8] B.F.G. Katz, "Boundary element method calculation of individual head-related transfer function. I. Rigid model calculation", *Journal of Acoustical Society of America* **110**, 2440-2448 (2001)

[9] B.F.G. Katz, "Boundary element method calculation of individual head-related transfer function. II. Impedance effects and comparison to real measurements", *Journal of Acoustical Society of America* **110**, 2449-2455 (2001)